

# Titanium nitride as a plasmonic material for visible and near-infrared wavelengths

Gururaj V. Naik,<sup>1</sup> Jeremy L. Schroeder,<sup>2</sup> Xingjie Ni,<sup>1</sup> Alexander V. Kildishev,<sup>1</sup> Timothy D. Sands,<sup>1,2</sup> and Alexandra Boltasseva<sup>1,3,\*</sup>

<sup>1</sup>*School of Electrical & Computer Engineering and Birck Nanotechnology Center, Purdue University, West Lafayette, Indiana 47907, USA*

<sup>2</sup>*School of Materials Engineering and Birck Nanotechnology Center, Purdue University, West Lafayette, Indiana 47907, USA*

<sup>3</sup>*DTU Fotonik, Technical University of Denmark, Lyngby 2800, Denmark*

[\\*aeb@purdue.edu](mailto:aeb@purdue.edu)

**Abstract:** The search for alternative plasmonic materials with improved optical properties, easier fabrication and integration capabilities over those of the traditional materials such as silver and gold could ultimately lead to real-life applications for plasmonics and metamaterials. In this work, we show that titanium nitride could perform as an alternative plasmonic material in the visible and near-infrared regions. We demonstrate the excitation of surface-plasmon-polaritons on titanium nitride thin films and discuss the performance of various plasmonic and metamaterial structures with titanium nitride as the plasmonic component. We also show that titanium nitride could provide performance that is comparable to that of gold for plasmonic applications and can significantly outperform gold and silver for transformation-optics and some metamaterial applications in the visible and near-infrared regions.

© 2012 Optical Society of America

**OCIS codes:** (160.3918) Metamaterials; (250.5403) Plasmonics.

---

## References and links

1. W. Barnes, A. Dereux, and T. Ebbesen, "Surface plasmon subwavelength optics," *Nature* **424**, 824–830 (2003).
2. S. Lal, S. Link, and N. Halas, "Nano-optics from sensing to waveguiding," *Nat. Photonics* **1**, 641–648 (2007).
3. D. Smith, J. Pendry, and M. Wiltshire, "Metamaterials and negative refractive index," *Science* **305**, 788–792 (2004).
4. W. Cai and V. Shalaev, *Optical Metamaterials: Fundamentals and Applications* (Springer Verlag, 2009).
5. J. Pendry, D. Schurig, and D. Smith, "Controlling electromagnetic fields," *Science* **312**, 1780–1782 (2006).
6. C. Soukoulis, S. Linden, and M. Wegener, "Physics: negative refractive index at optical wavelengths," *Science* **315**, 47–49 (2007).
7. V. Shalaev, "Transforming light," *Science* **322**, 384–386 (2008).
8. J. Pendry, "Negative refraction makes a perfect lens," *Phys. Rev. Lett.* **85**, 3966–3969 (2000).
9. Z. Jacob, L. Alekseyev, and E. Narimanov, "Optical Hyperlens: Far-field imaging beyond the diffraction limit," *Opt. Express* **14**, 8247–8256 (2006).
10. S. Ramakrishna, J. Pendry, M. Wiltshire, and W. Stewart, "Imaging the near field," *J. Mod. Opt.* **50**, 1419–1430 (2003).
11. W. Cai, U. Chettiar, A. Kildishev, and V. Shalaev, "Optical cloaking with metamaterials," *Nat. Photonics* **1**, 224–227 (2007).
12. A. Kildishev and V. Shalaev, "Engineering space for light via transformation optics," *Opt. Lett.* **33**, 43–45 (2008).
13. E. Narimanov and A. Kildishev, "Optical black hole: Broadband omnidirectional light absorber," *Appl. Phys. Lett.* **95**, 041106 (2009).
14. N. Fang, H. Lee, C. Sun, and X. Zhang, "Sub-diffraction-limited optical imaging with a silver superlens," *Science* **308**, 534–537 (2005).

15. Z. Liu, H. Lee, Y. Xiong, C. Sun, and X. Zhang, "Far-field optical hyperlens magnifying sub-diffraction-limited objects," *Science* **315**, 1686–1686 (2007).
16. V. Shalaev, W. Cai, U. Chettiar, H. Yuan, A. Sarychev, V. Drachev, and A. Kildishev, "Negative index of refraction in optical metamaterials," *Opt. Lett.* **30**, 3356–3358 (2005).
17. G. Dolling, M. Wegener, C. Soukoulis, and S. Linden, "Negative-index metamaterial at 780 nm wavelength," *Opt. Lett.* **32**, 53–55 (2007).
18. D. Schurig, J. Mock, B. Justice, S. Cummer, J. Pendry, A. Starr, and D. Smith, "Metamaterial electromagnetic cloak at microwave frequencies," *Science* **314**, 977–980 (2006).
19. T. Ergin, N. Stenger, P. Brenner, J. Pendry, and M. Wegener, "Three-dimensional invisibility cloak at optical wavelengths," *Science* **328**, 337–339 (2010).
20. A. Boltasseva and H. Atwater, "Low-loss plasmonic metamaterials," *Science* **331**, 290–291 (2011).
21. P. Johnson and R. Christy, "Optical constants of the noble metals," *Phys. Rev. B* **6**, 4370–4379 (1972).
22. G. Naik and A. Boltasseva, "Semiconductors for plasmonics and metamaterials," *Phys. Status Solidi (RRL)* **4**, 295–297 (2010).
23. P. West, S. Ishii, G. Naik, N. Emani, V. Shalaev, and A. Boltasseva, "Searching for better plasmonic materials," *Laser Photonics Rev.* **4**, 795–808 (2010).
24. M. Noginov, L. Gu, J. Livenere, G. Zhu, A. Pradhan, R. Mundle, M. Bahoura, Y. Barnakov, and V. Podolskiy, "Transparent conductive oxides: Plasmonic materials for telecom wavelengths," *Appl. Phys. Lett.* **99**, 021101 (2011).
25. A. Frölich and M. Wegener, "Spectroscopic characterization of highly doped ZnO films grown by atomic-layer deposition for three-dimensional infrared metamaterials," *Opt. Mater. Express* **1**, 883–889 (2011).
26. T. Minami, "New n-type transparent conducting oxides," *MRS Bull.* **25**, 38–44 (2000).
27. G. Naik, J. Kim, and A. Boltasseva, "Oxides and nitrides as alternative plasmonic materials in the optical range," *Opt. Mater. Express* **1**, 1090–1099 (2011).
28. D. Park, T. Cha, K. Lim, H. Cho, T. Kim, S. Jang, Y. Suh, V. Misra, I. Yeo, J. Roh, J. Park, and H. Yoon, "Robust ternary metal gate electrodes for dual gate CMOS devices," in *Electron Devices Meeting, 2001. IEDM Technical Digest. International* (IEEE, 2001), pp. 30–36.
29. L. Hiltunen, M. Leskela, M. Makela, L. Niinisto, E. Nykanen, and P. Soininen, "Nitrides of titanium, niobium, tantalum and molybdenum grown as thin films by the atomic layer epitaxy method," *Thin Solid Films* **166**, 149–154 (1988).
30. S. Aouadi and M. Debessai, "Optical properties of tantalum nitride films fabricated using reactive unbalanced magnetron sputtering," *J. Vac. Sci. Technol. A* **22**, 1975–1979 (2004).
31. P. Patsalas and S. Logothetidis, "Optical, electronic, and transport properties of nanocrystalline titanium nitride thin films," *J. Appl. Phys.* **90**, 4725–4734 (2001).
32. B. Johansson, J. Sundgren, J. Greene, A. Rockett, and S. Barnett, "Growth and properties of single crystal TiN films deposited by reactive magnetron sputtering," *J. Vac. Sci. Technol. A* **3**, 303–307 (1985).
33. W.-C. Chen, Y.-R. Lin, X.-J. Guo, and S.-T. Wu, "Heteroepitaxial TiN of Very Low Mosaic Spread on Al<sub>2</sub>O<sub>3</sub>," *Jpn. J. Appl. Phys.* **42**, 208–212 (2003).
34. V. Drachev, U. Chettiar, A. Kildishev, H. Yuan, W. Cai, and V. Shalaev, "The Ag dielectric function in plasmonic metamaterials," *Opt. Express* **16**, 1186–1195 (2008).
35. P. Berini, "Figures of merit for surface plasmon waveguides," *Opt. Express* **14**, 13030–13042 (2006).
36. C. Davis, D. McKenzie, and R. McPhedran, "Optical properties and microstructure of thin silver films," *Opt. Commun.* **85**, 70–82 (1991).
37. Y. Yagil, P. Gadenne, C. Julien, and G. Deutscher, "Optical properties of thin semicontinuous gold films over a wavelength range of 2.5 to 500  $\mu\text{m}$ ," *Phys. Rev. B* **46**, 2503–2511 (1992).
38. K. Chen, V. Drachev, J. Borneman, A. Kildishev, and V. Shalaev, "Drude relaxation rate in grained gold nanoantennas," *Nano Lett.* **10**, 916–922 (2010).
39. X. Ni, Z. Liu, and A. V. Kildishev, "PhotonicsDB: Optical Constants," <http://nanohub.org/resources/PhotonicsDB>. (doi:10254/nanohub-r3692.10) (2010).
40. J. A. Dionne, L. A. Sweatlock, H. A. Atwater, and A. Polman, "Plasmon slot waveguides: Towards chip-scale propagation with subwavelength-scale localization," *Phys. Rev. B* **73**, 035407 (2006).
41. S. Maier, *Plasmonic Nanoguides and Circuits* (Pan Stanford Publishing Pte. Ltd., 2009).
42. M. Cortie, J. Giddings, and A. Dowd, "Optical properties and plasmon resonances of titanium nitride nanostructures," *Nanotechnol.* **21**, 115201 (2010).
43. Z. Jacob, I. Smolyaninov, and E. Narimanov, "Broadband Purcell effect: Radiative decay engineering with metamaterials," Arxiv preprint arXiv:0910.3981 (2009).
44. Z. Jacob, J.-Y. Kim, G. Naik, A. Boltasseva, E. Narimanov, and V. Shalaev, "Engineering photonic density of states using metamaterials," *Appl. Phys. B* **100**, 215–218 (2010).
45. G. Naik and A. Boltasseva, "A comparative study of semiconductor-based plasmonic metamaterials," *Metamaterials* **5**, 1–7 (2011).
46. G. Naik, J. Liu, A. Kildishev, V. Shalaev, and A. Boltasseva, "Negative refraction in Al:ZnO/ZnO metamaterial in the near-infrared," Arxiv preprint arXiv:1110.3231 (2011).

47. A. Hoffman, L. Alekseyev, S. Howard, K. Franz, D. Wasserman, V. Podolskiy, E. Narimanov, D. Sivco, and C. Gmachl, "Negative refraction in semiconductor metamaterials," *Nat. Mater.* **6**, 946–950 (2007).
  48. V. Podolskiy and E. Narimanov, "Strongly anisotropic waveguide as a nonmagnetic left-handed system," *Phys. Rev. B* **71**, 201101 (2005).
  49. J. Elser, V. Podolskiy, I. Salakhutdinov, and I. Avrutsky, "Nonlocal effects in effective-medium response of nanolayered metamaterials," *Appl. Phys. Lett.* **90**, 191109 (2007).
  50. S. Maier, *Plasmonics: Fundamentals and Applications* (Springer Verlag, 2007).
  51. A. Hibbins, J. Sambles, and C. Lawrence, "Surface plasmon-polariton study of the optical dielectric function of titanium nitride," *J. Mod. Opt.* **45**, 2051–2062 (1998).
  52. X. Ni, Z. Liu, A. Boltasseva, and A. Kildishev, "The validation of the parallel three-dimensional solver for analysis of optical plasmonic bi-periodic multilayer nanostructures," *Appl. Phys. A* **100**, 365–374 (2010).
- 

## 1. Introduction

Plasmonics [1,2] and metamaterials (MMs) [3,4] have advanced enormously in the past decade bringing about a paradigm shift from conventional photonics. Together with transformation optics (TO) [5–7], plasmonics and MMs have produced a new set of ideas such as negative refractive index materials [8], nanoscale imaging devices [9,10], invisibility cloaks [11] and light concentrators [12,13], thus paving the way for the realization of devices with unprecedented functionalities [14–19]. Although the experimental realizations of these devices serve as exciting demonstrations of the phenomena, practical applications thus far are limited. One of the major challenges hindering MM and TO applications in real devices is the large loss coming from the plasmonic components of these devices [20]. Conventional plasmonic materials such as gold and silver exhibit excessive losses at optical frequencies [21], making them less suitable for real-world devices. In addition to the problem of loss, another major issue associated with the use of conventional metals in device applications is that the real parts of metal permittivities are too large in magnitude to be useful for many TO and MM devices [12]; ideally, the permittivity of the plasmonic material in a device would be adjustable. Another important factor is the ease of integration of the plasmonic material with standard semiconductor fabrication processes. The easy integration of plasmonic devices could allow the leveraging of standard semiconductor manufacturing technologies and processes for combining plasmonic materials with semiconductor devices.

In the search for better plasmonic materials, transparent conducting oxides (TCOs) were proposed as good alternatives to gold and silver in the near-infrared (near-IR) range [22–25]. However, TCOs cannot be plasmonic (i.e. exhibiting metallic properties) at visible wavelengths because the carrier concentration is limited to around  $10^{21} \text{ cm}^{-3}$  [26]. Transition-metal nitrides such as titanium nitride and zirconium nitride can have carrier concentrations higher than those achievable in TCOs [27]. Despite the fact that the optical losses are not smaller than those of noble metals, the magnitude of the real permittivity of these metal nitrides in the visible range is much smaller than that of noble metals owing to the smaller carrier concentration. Additionally, the optical properties of these metal nitrides may be tuned, unlike the case for noble metals, simply by changing the processing conditions [27]. Another major advantage of titanium nitride and zirconium nitride is that they offer easy fabrication and integration with standard silicon manufacturing processes [28]. All of the above factors make transition metal nitrides promising alternative plasmonic materials in the visible and near-IR regions.

This paper focuses on titanium nitride for plasmonic and metamaterial applications in the visible and near-IR regions. We present the optimization of processing conditions as well as material and optical characterization results for TiN thin films. We also provide a comparative study of the performance of various plasmonic and metamaterial devices with TiN as the plasmonic material. The paper concludes with the demonstration of the plasmonic properties of TiN thin films by exciting surface plasmon polaritons (SPPs) on these films.

## 2. Titanium nitride: deposition and characterization

Transition metal nitrides such as TiN are ceramic materials that are non-stoichiometric. In other words, the composition and hence the optical properties depend significantly on the preparation method and conditions. Some of these nitrides possess metallic properties at visible wavelengths because of large free carrier concentrations ( $\approx 10^{22} \text{cm}^{-3}$ ) [29–31]. High interband losses make many of these compounds unattractive for plasmonic applications. Titanium nitride, however, exhibits smaller interband losses in the red part of the visible spectrum and a small negative real permittivity [31]. It is therefore a material of significant interest for plasmonic applications in the visible and near-IR ranges.

Thin films of titanium nitride were deposited on glass or c-sapphire substrates by DC reactive magnetron sputtering (PVD Products Inc.) from a 99.995% titanium target in an argon-nitrogen environment. The base pressure within the chamber before deposition was  $2 \times 10^{-7}$  Torr. The films were deposited at a pressure of 5 mTorr with varying flow ratios of argon and nitrogen (Ar (sccm):N<sub>2</sub> (sccm) of 4:6, 2:8 and 0:10). The sputtering power was held constant for all depositions at 200 W (DC) and the target-substrate distance was 8 cm. The deposition rate was approximately 25 Å/min and about 30 nm thick films were deposited. The substrate temperature during deposition was held at 300 °C or 500 °C. The resulting films were characterized by a variable angle spectroscopic ellipsometer (V-VASE, J.A. Woollam Co.) in the near-IR, visible and near-UV wavelength ranges. A Drude-Lorentz (with three Lorentz oscillators) model provided a good fit to the ellipsometric measurements. The Drude part of the model captures the part of the optical response arising from free carriers, while the Lorentz oscillators account for the interband losses. Figure 1 shows the dielectric functions retrieved for three TiN films deposited at 300 °C on c-sapphire substrates with different flow ratios of argon and nitrogen. Note that the Drude damping of the carriers does not vary significantly among the three films. However, the unscreened plasma frequency increases slightly for the film deposited at a flow ratio of 2:8 (Ar:N<sub>2</sub>), which results in higher loss compared to the other films.

The influence of the substrate temperature on the optical properties of these films was studied by depositing TiN films at substrate temperatures of 300 °C and 500 °C with the Ar:N<sub>2</sub> flow ratio fixed at 4:6. Figure 2 shows the dielectric function extracted for these two films. Clearly, the film deposited at the higher temperature shows lower loss.

The optical properties of TiN thin films also depend strongly on the substrate on which they are grown. Substrates such as sapphire and MgO provide lattice matching and promote epitaxial growth [32, 33], leading to crystalline films and thereby reducing optical losses [34]. Substrates such as glass do not provide lattice matching and polycrystalline films are obtained which can have higher losses due to additional carrier scattering. The optical properties of a TiN film grown on c-sapphire and glass are shown in Fig. 3. The film grown on glass shows lower carrier concentration and higher losses than the film grown on c-sapphire. In order to verify if c-sapphire allows epitaxial growth of TiN films, X-ray diffraction (Phillips X'Pert Pro) measurements were performed. The diffraction intensity plot for TiN thin films on c-sapphire substrate is shown in Fig. 4. The  $2\theta - \omega$  plot shows two peaks corresponding to the 111 reflection from TiN and the 0006 reflection from sapphire substrate. TiN film on c-sapphire grows essentially in the [111] direction. Further, the epitaxial growth of TiN on c-sapphire is confirmed by performing an asymmetric-phi scan. In this measurement, the x-ray detector ( $2\theta$ ) and the incidence angle at the sample ( $\omega$ ) are fixed at values corresponding to the 200 reflection. The off-plane tilt of the sample ( $\chi$ ) is set to 54.7 degrees corresponding to the interplanar angle between (200) and (111) planes. Epitaxial growth would be evidenced by peaks corresponding to three 200 reflections when the sample is rotated by 360 degrees. The inset in Fig. 4 shows the result of an asymmetric-phi scan on a TiN film deposited on a c-sapphire substrate. The six sharp peaks observed in this measurement confirm multivariant epitaxial growth of TiN on

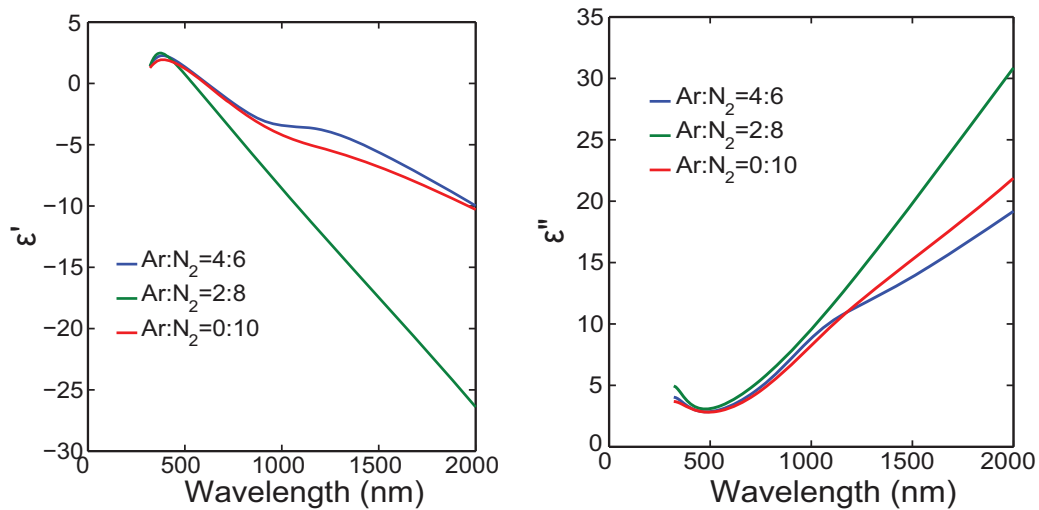


Fig. 1. Dielectric functions of sputter-deposited titanium nitride films retrieved by spectroscopic ellipsometry measurements. The films were deposited on c-sapphire substrates by DC reactive magnetron sputtering at 300 °C with different flow ratios (sccm:sccm) of argon and nitrogen.

c-sapphire.

Epitaxial growth of TiN thin films on c-sapphire produces films that have low roughness and are uniformly textured. In Fig. 5, we show representative atomic force microscope (AFM) and scanning electron micrograph (SEM) images of a TiN film on a c-sapphire substrate. The root-mean-square (rms) roughness of the film is measured to be about 0.4 nm as shown in Fig 5a. Although the film is smoother than a polycrystalline film, the boundaries between domains of epitaxial variants of cubic TiN introduce a degree of roughness.

### 3. Plasmonic and metamaterial applications

In this section, we consider TiN as a plasmonic building block for different applications such as SPP waveguides, localized surface plasmon resonance (LSPR) devices, hyperbolic MMs, and general transformation optics devices. The figures-of-merit of these devices with TiN as plasmonic component are evaluated and compared against their elemental metal based counterparts.

#### 3.1. Plasmonic applications

An SPP propagating along a single metal/air interface is characterized by two important parameters: the propagation length (defined as the 1/e field-decay length along the direction of propagation) and the confinement width (the 1/e field-decay width on each side of the interface) [35]. There is a trade-off between these parameters such that weaker confinement results in a longer propagation length and vice versa. In general, the trade-off is very sensitive to losses in the metal and decreases sharply with higher damping losses. Since it has the lowest Drude damping, silver offers the best SPP characteristics. However, problems in fabricating thin films of silver and its chemical reactivity in air preclude it from being useful for some applications [34, 36]. Gold is better due its chemical stability, but it poses other problems arising from nanofabrication such as poor adhesion to substrates and the formation of percolating or

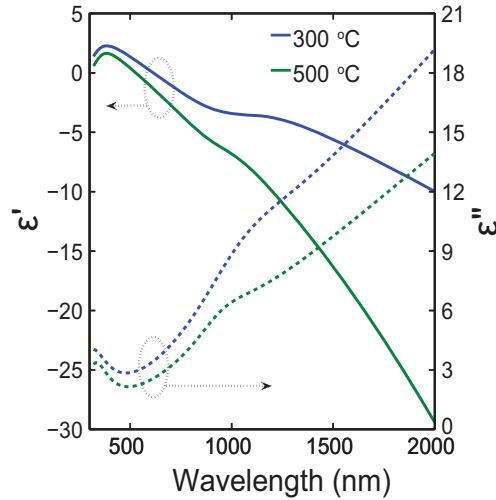


Fig. 2. Dielectric functions of titanium nitride films deposited at 300 °C and 500 °C retrieved by spectroscopic ellipsometry measurements. The films were deposited with the flow ratio of argon and nitrogen set to 4:6.

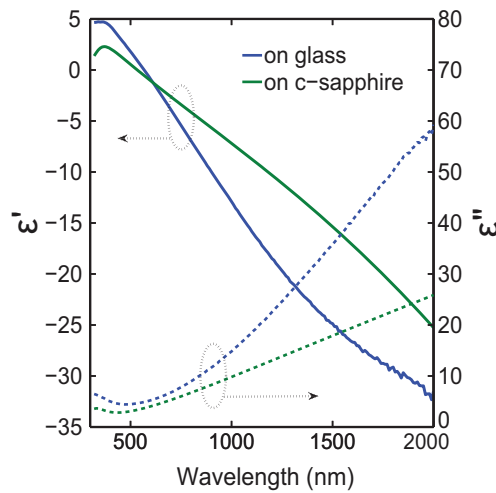


Fig. 3. Dielectric functions of titanium nitride films deposited at 300 °C on glass and c-sapphire substrates.

semicontinuous films when the thickness is around 10 nm or lower [37, 38]. Such problems arising from the growth and morphology of gold films result in additional optical losses, which can be described by a phenomenological quantity called the loss factor [34, 38]. This loss factor directly multiplies the Drude-damping rate and increases the imaginary part of the permittivity for values greater than unity. In the following comparative study, the optical properties of noble metals are derived from the well-known work by Johnson and Christy (JC) [21, 39] and the loss factor is applied onto this data.

Figure 6 shows the propagation lengths and confinements for SPPs along the interface between air and TiN, air and gold, and air and gold with a loss factor of 3.5. Note that TiN gives a slightly better confinement than gold, but the propagation length for TiN is smaller than that for

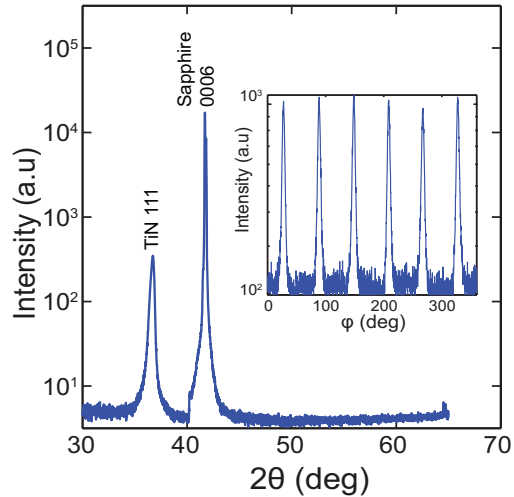


Fig. 4. X-ray diffraction plot showing the diffraction intensity from a TiN thin film grown on c-sapphire. The peaks in the intensity correspond to the crystal planes annotated. The inset shows the intensity plot for an asymmetric-phi scan with  $2\theta$  set to the 200 reflection of TiN and off-plane tilt angle ( $\chi$ ) set to 54.7 degrees corresponding to interplanar angle between (111) and (200) planes.

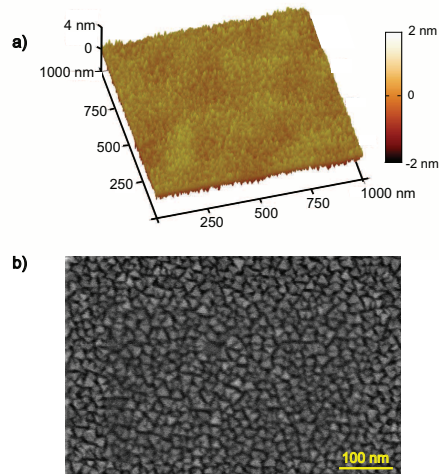


Fig. 5. Characterization of 30 nm thick TiN film deposited on a c-sapphire substrate. a) Atomic force microscope (AFM) image b) Scanning electron micrograph.

gold. The characteristics of TiN resemble that of gold with a loss factor of 3.5. As a comparison point, a loss factor of 3.5 or higher is commonly observed in nanopatterned gold structures.

Instead of the simple case of SPPs propagating along a single interface, more complicated designs such as a metal-insulator-metal (MIM) waveguide geometry with TiN are also worth considering [40]. The MIM configuration allows confinement of a significant portion of the electromagnetic field within the insulator and, hence, the propagation length of SPPs in this configuration is a fair index for comparing the performance of different plasmonic material

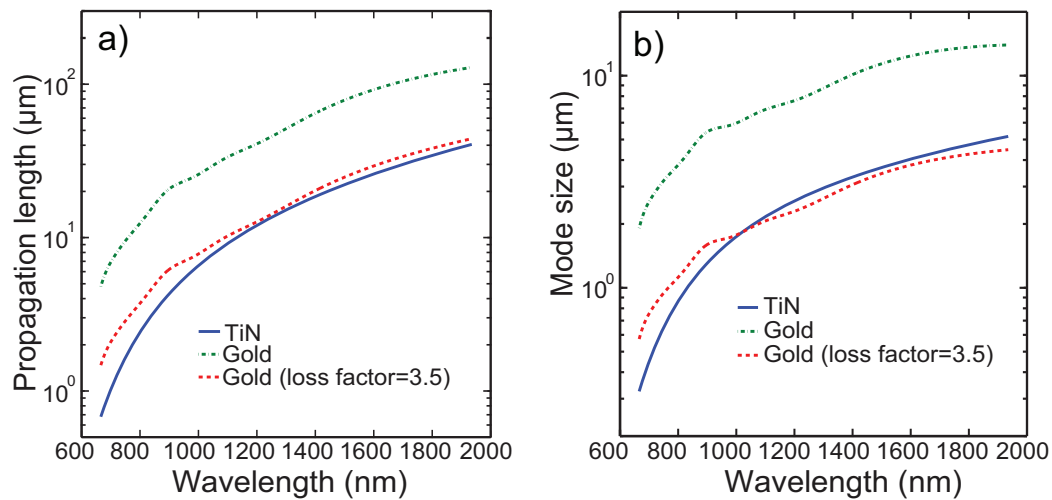


Fig. 6. Comparison of the performance characteristics of SPP waveguides formed by the interface of air with TiN-, gold (JC)- and gold with loss factor of 3.5: a) Propagation length (1/e field decay length along the propagation direction) b) Confinement width (1/e field decay widths on each side normal to the interface).

systems. Figure 7 shows the propagation lengths calculated [41] for the lowest order symmetric SPP mode in an MIM waveguide with a 300 nm air gap as the insulator and TiN or gold as the metal. The propagation length is smaller for the case of TiN compared to gold with a unity loss factor. However, the propagation length of a TiN waveguide is comparable to that of gold with a loss factor of 3.5.

In addition to propagating modes, localized surface plasmon resonance (LSPR) modes are useful in many sensing applications where localized field enhancement is of great importance [2]. Metal nanoparticles can support LSPR modes and enable local-field enhancement. The field enhancements at the surface of TiN and gold nanospheres calculated using the quasistatic dipole approximation are shown in Fig. 8. The resonance wavelength (which corresponds to the peak field enhancement) for TiN nanospheres is red-shifted compared to gold owing to TiN's smaller absolute real permittivity value [42]. The magnitude of field enhancement in TiN nanospheres is slightly smaller than that of gold, but the overall performance of each material is comparable, making TiN a realistic alternative plasmonic material for LSPR applications.

### 3.2. Hyperbolic metamaterials and transformation optics

MMs with hyperbolic dispersion are receiving increasing attention from researchers because of their unique properties such as the propagation of extremely high-k waves [9] and a broadband singularity in the photonic-density-of-states (PDOS) [43]. These properties have resulted in devices such as the hyperlens [9] and phenomena such as engineering the spontaneous emission rate [44], both of which have useful applications in quantum optics. Hyperbolic MMs (HMMs) can be easily fabricated by stacking alternating, sub-wavelength layers of metal and dielectric materials. For example, the first demonstration of a hyperlens used alternating layers of silver and alumina [15]. However, such a material system works well only in the near-UV where the performance of silver is best-suited for HMMs. In the visible spectrum, neither gold nor silver can produce high-performance HMMs [45, 46]. To compare the performance, we adopt the

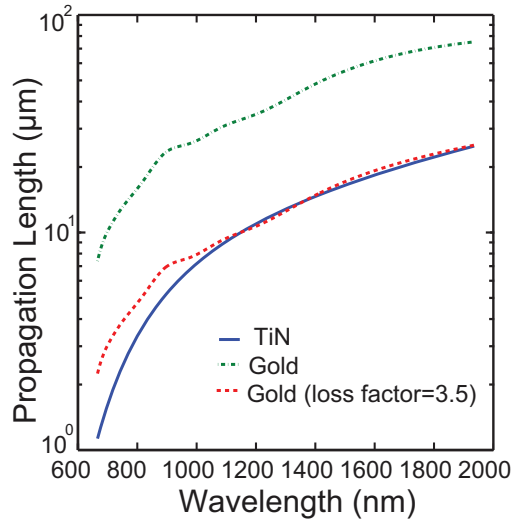


Fig. 7. Propagation length of the lowest order symmetric SPP mode in a metal/air/metal waveguide with an air gap of 300 nm for different metals: TiN, gold (JC) and gold with loss factor of 3.5.

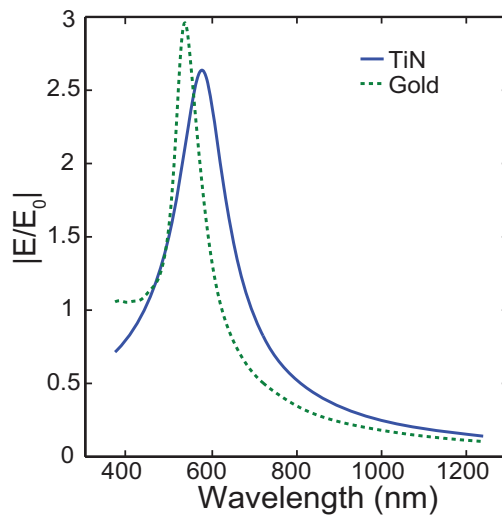


Fig. 8. Localized-surface-plasmon applications: Calculated field enhancement at the surface of TiN and gold nanospheres calculated using quasistatic dipole approximation.

figure-of-merit from [47] as  $Re\{\beta_{\perp}\}/Im\{\beta_{\perp}\}$ , where  $\beta_{\perp}$  is the propagation vector of an electromagnetic wave along the direction perpendicular to the plane of the metal/dielectric layers. Figure 9 shows the figures-of-merit of HMMs formed by alternating layers of silver/alumina, gold/alumina and TiN/AlN. Here, the calculations of figure-of-merit are based on standard effective medium approximation of the metal/dielectric stack for a metal filling fraction of 50% [48, 49]. Clearly, the TiN system outperforms the metal based systems in the red part of the visible spectrum. For wavelengths shorter than 500 nm, TiN is not plasmonic; therefore, the figure-of-merit values are shown only for wavelengths longer than 500 nm. TiN not only

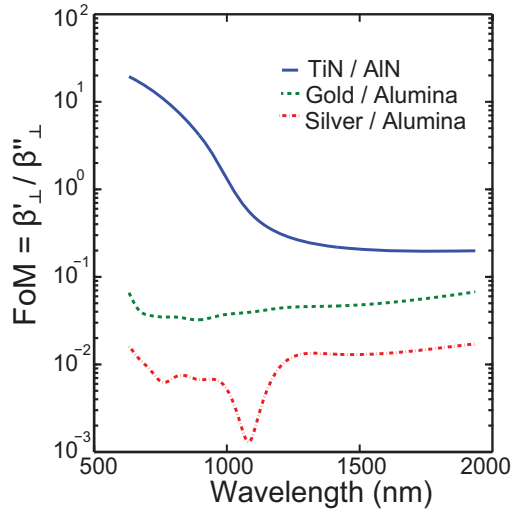


Fig. 9. Figures-of-merit for HMMs formed by alternating, sub-wavelength layers of different metal/dielectric combinations (TiN/AlN, silver/alumina and gold/alumina).

outperforms in its performance, but also provides an additional advantage in the fabrication of ultra-thin layers. Ultra-thin layers are necessary for producing truly binary HMM structure and TiN, unlike metals can be grown as an ultra-thin epitaxial layer.

In general, transformation optics devices often require plasmonic components with real permittivity values that are on the order of unity. While none of the conventional metals satisfy this condition, titanium nitride does meet this criterion and is therefore a suitable material that could enable transformation optics in the visible range. As a comparison, the dielectric functions of TiN and bulk, conventional metals are plotted in Fig. 10. The figure clearly shows the disadvantage of conventional metals in terms of the real part of permittivity. However, the imaginary part of permittivity, which signifies the losses in the material, is the lowest in the case of silver. TiN is better than gold only for longer wavelengths. In practical applications, it is rather difficult to obtain low, bulk-like losses in designs using silver because of problems such as surface roughness, grain-boundary scattering and corrosion. Also, forming ultra-thin layers of silver or gold is difficult. On the contrary, TiN does not possess such difficulties and forms a better materials choice than conventional metals for TO applications.

#### 4. Excitation of SPPs

In order to demonstrate the plasmonic behavior of TiN, we studied the properties of SPPs at the interface of TiN and a dielectric. Since SPPs have momentum that is larger than that supported in the dielectric, direct excitation of SPP modes is not possible. However, many different techniques can be employed to excite SPPs on an interface [50]. In this work we demonstrate the excitation of SPPs on 30-nm-thick films of TiN using the grating coupling technique [51]. Initially, about 110 nm of an electron-beam resist (ZEP) is spin-coated on the TiN film and patterned into dielectric gratings with a periodicity of  $1.5 \mu\text{m}$  (see inset of Fig. 11). The angular reflectance of this structure was measured using a variable-angle spectroscopic ellipsometer (J.A. Woollam Co.). The incident beam was TM polarized, and the gratings were aligned parallel to the incident magnetic field. The angular reflectance measured at two different wavelengths in the near-IR range is shown Fig. 11. The dips in reflectance observed around 30 and 25 degrees for wavelengths of 900 and 1000 nm respectively correspond to the excitation of

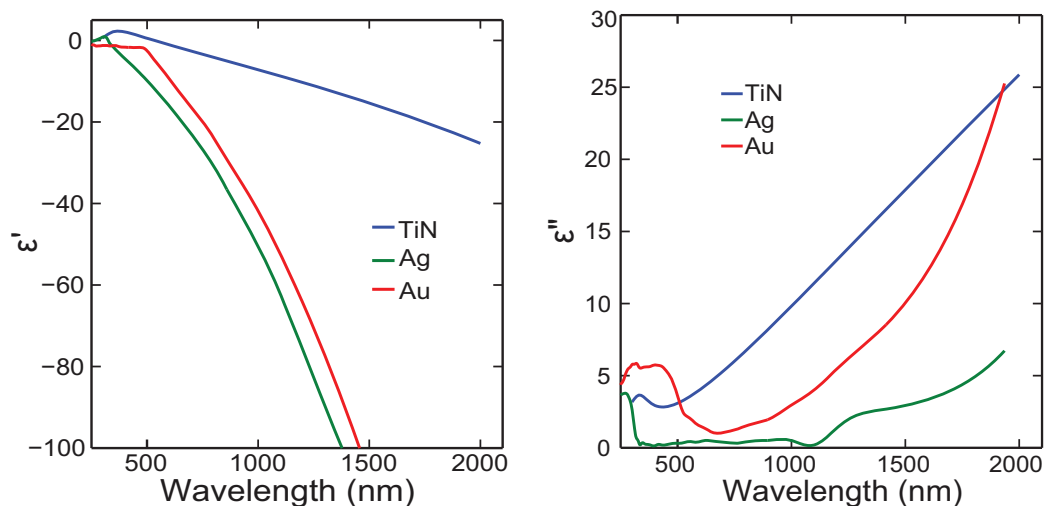


Fig. 10. Dielectric function of TiN in comparison with conventional plasmonic materials: gold and silver (data adapted from JC [21, 39]).

SPPs along the interface. We confirmed that this observed behavior arises due to SPP excitation by computing the SPP dispersion curve for a TiN/ZEP interface and the momentum mismatch between the SPP-curve and the light line of the dielectric. The additional momentum required to couple SPPs is provided exactly by the grating at these angles of incidence, producing a dip in the observed reflectance. The reflectance dip is shallow owing to the weak coupling offered by the thin dielectric grating. A thicker dielectric grating or a plasmonic grating formed by patterning the TiN film could overcome this problem and provide stronger SPP coupling.

The observed optical phenomenon was also verified through simulations using the spatial harmonic analysis (SHA) method [52]. The optical constants of the TiN film and dielectric polymer (ZEP) for the simulations were obtained from ellipsometry measurements as stated above. The thickness of the dielectric gratings was adjusted from the measured value within 5% to match the experimental curves. The results of the calculations are shown in Fig. 11 for two different excitation wavelengths. The calculations match the experiments reasonably well, confirming the excitation of SPPs on the TiN film.

## 5. Conclusion

We have shown that titanium nitride can serve as an alternative plasmonic material for plasmonic and metamaterial applications in the visible and near-IR frequencies. We showed that titanium nitride, being a non-stoichiometric compound, exhibits process-dependent properties. Thin TiN films deposited on c-sapphire substrates showed multivariant epitaxial growth and formed smooth films. Our comparative study of TiN and conventional plasmonic materials suggested that TiN offers comparable performance for plasmonic applications and significantly better performance for transformation optics and metamaterial devices such as hyperbolic metamaterial devices. Titanium nitride was shown to support SPPs in the near-IR range by using dielectric gratings to excite SPPs on TiN/dielectric interfaces. An inherent advantage of TiN is that it is compatible with standard silicon manufacturing processes, unlike gold and silver. This could allow easy integration of silicon electronics with plasmonics. Titanium nitride also overcomes many other nanofabrication problems associated with gold and silver, making it a

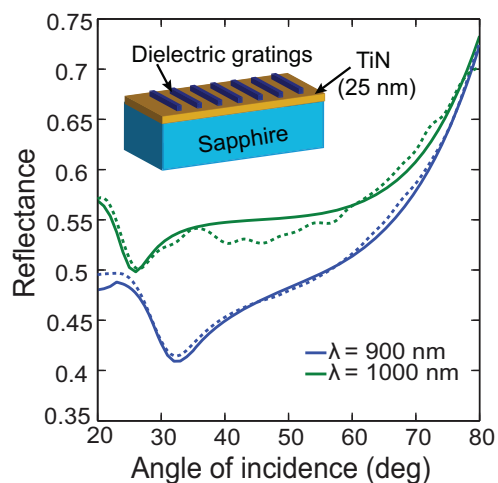


Fig. 11. Angular reflectance of dielectric (ZEP, electron-beam resist) gratings formed on top of a 30 nm thick film of TiN. The inset shows the geometry of the structure. The measured (solid lines) and calculated (dashed lines) reflectances are plotted against angle of incidence for two different wavelengths.

technologically important alternative plasmonic material.

### Acknowledgments

We thank Prof. Vladimir M. Shalaev for useful discussions. This work was supported in part by ARO grant number W911NF-11-1-0359 and ONR-MURI grant N00014-10-1-0942. Dr. A.V. Kildishev was partially supported by the AFRL Materials and Manufacturing Directorate Applied Metamaterials Program.